

## Follow-the-Leader Guidance, Navigation, and Control of Surface Vessels

### Design and Experiments

Piaggio, Benedetto; Garofano, Vittorio; Donnarumma, Silvia; Alessandri, Angelo; Negenborn, Rudy; Martelli, Michele

**DOI**

[10.1109/JOE.2023.3292422](https://doi.org/10.1109/JOE.2023.3292422)

**Publication date**

2023

**Document Version**

Final published version

**Published in**

IEEE Journal of Oceanic Engineering

**Citation (APA)**

Piaggio, B., Garofano, V., Donnarumma, S., Alessandri, A., Negenborn, R., & Martelli, M. (2023). Follow-the-Leader Guidance, Navigation, and Control of Surface Vessels: Design and Experiments. *IEEE Journal of Oceanic Engineering*, 48(4), 997-1008. <https://doi.org/10.1109/JOE.2023.3292422>

**Important note**

To cite this publication, please use the final published version (if applicable).  
Please check the document version above.

**Copyright**

Other than for strictly personal use, it is not permitted to download, forward or distribute the text or part of it, without the consent of the author(s) and/or copyright holder(s), unless the work is under an open content license such as Creative Commons.

**Takedown policy**

Please contact us and provide details if you believe this document breaches copyrights.  
We will remove access to the work immediately and investigate your claim.






***Green Open Access added to TU Delft Institutional Repository***

***'You share, we take care!' - Taverne project***

**<https://www.openaccess.nl/en/you-share-we-take-care>**

Otherwise as indicated in the copyright section: the publisher is the copyright holder of this work and the author uses the Dutch legislation to make this work public.

# Follow-the-Leader Guidance, Navigation, and Control of Surface Vessels: Design and Experiments

Benedetto Piaggio , Vittorio Garofano, Silvia Donnarumma , Angelo Alessandri , *Senior Member, IEEE*, Rudy Negenborn , and Michele Martelli 

**Abstract**—A novel follow-the-leader approach for azimuth-driven vessels is devised and experimentally tested in a model-scale outdoor scenario. The vessels are equipped with global navigation satellite and inertial navigation systems. A line-of-sight algorithm ensures the yaw-check ability of the follower vessel along the leader’s path, while a speed-regulation allows to track its velocity. Track generation, guidance, navigation, and control modules are designed and assembled to be executed on-board in real time. The results of an outdoor experimental campaign are illustrated to show the effectiveness of the proposed approach.

**Index Terms**—Azimuth-drive propulsion, escort tugs, follow-the-leader control, line of sight (LOS), track keeping.

## I. INTRODUCTION

**M**OST of the operational life of sailing vessels consists in tracking a predetermined path in restricted and open waters, according to complex traffic management constraints and risks [1]. The capability of forming convoys and following a leading target-vessel within its wake is a valuable feature in both blue seas and busy/restricted areas, such as inland waterways and harbors [2]. In this scenario, the two main challenges are to steer, while keeping off-track tolerances, and to tune the speed according to the leader. Such objectives need to be reached with high accuracy and are crucial to safely exploit the viable inland waterways’ routes and minimize the sailing delays and accidents [3], [4].

Manuscript received 26 April 2021; revised 10 August 2022; accepted 11 May 2023. Date of publication 15 September 2023; date of current version 13 October 2023. This work was supported in part by the ResearchLab on Autonomous Shipping (RAS) of the Delft University of Technology, in part by the COMPASS Lab of the University of Genoa, and in part by the INTERREG North Sea Region project AVATAR “Sustainable urban freight transport with autonomous zero-emission vessels.” Preliminary work for this paper was presented at IMarEST International Ship Control Systems Symposium 2020 (iSCSS) [DOI: 10.24868/issn.2631-8741.2020.004]. (*Corresponding author: Benedetto Piaggio.*)

**Associate Editor: J. Sousa.**

Benedetto Piaggio, Silvia Donnarumma, and Michele Martelli are with the Department of Naval Architecture and Marine, Electrical, Electronic, Telecommunications Engineering, Polytechnic School of Genoa University, 16145 Genoa, Italy (e-mail: benedetto.piaggio@unige.it; silvia.donnarumma@unige.it; michele.martelli@unige.it).

Vittorio Garofano and Rudy Negenborn are with the Department of Maritime and Transport Technology, Delft University of Technology, 2628 CN Delft, The Netherlands (e-mail: v.garofano@tudelft.nl; r.r.negenborn@tudelft.nl).

Angelo Alessandri is with the Department of Mechanical, Energetics, Management and Transportation Engineering (DIME), Polytechnic School of Genoa University, 16145 Genoa, Italy (e-mail: angelo.alessandri@unige.it).

Digital Object Identifier 10.1109/JOE.2023.3292422

A big amount of information is required to actually maneuver a vessel and simultaneously follow a leading ship, thus making it a challenging task, even for the most expert bridge officer, who is also responsible to account for a lot of sensor data. In this work, an approach to the follow-the-leader control for azimuth-driven surface vessels is presented by relying on flexible  $0^\circ$ – $360^\circ$  thrust allocation and manoeuvring capabilities. These features turn out to be ideal for both work vessels, such as azimuth stern drive tugs, offshore supply vessels (z-drive ducted propellers), and passenger vessels (ducted or podded propellers), which all install azimuthing propulsion and control units at the stern regions [5], [6]. Such ships approach restricted/inland areas and harbors without the need for external assistance. The class of azimuth-driven vessels indeed represents the most competitive solution in handling steering vessels at both low and high-speed, and thus attracted the prime interest of the authors.

The ability to follow a moving target along its route meets the most restrictive needs of sailing in crowded and confined waters where traffic management is crucial for unmanned vehicles, thus raising a wide interest in the scientific community [7], [8]. The narrower the navigation lane, the greater the demand for precision in the guidance, navigation, and control (GNC) system. This dictates the requirement of gathering vessels in assembled and neat “train” convoys in compliance with the traffic control rules, i.e., multibody vessel platoons. The effective execution of such tasks is somehow preliminary toward autonomous inland waters or restricted waters navigation, which further motivates the present work.

Sophisticated path-following and tracking controllers for underactuated vehicles [9], and aided-navigation follow-the-leader control systems spread in the literature for both unmanned surface vehicles (USVs) [10], [11] and autonomous underwater vehicles [12]. Crucial aspects concern the robustness of the closed-loop system against model uncertainties, external disturbances, and input saturation constraints [13], and, in addition to this, formation control on straight and curvilinear paths [14], even with multiple vessels [15]. Complex scenarios consider distributed control for train formation as well [2], [16], [17]. Still recent efforts have been devoted to path following based on a line-of-sight (LOS) approach [18], [19] and extended Kalman filters (EKFs) based on a global navigation satellite system (GNSS) but without speed control [20]. Nevertheless, most of them are not fully contextualized with real vessel geometries and dynamics, and only a few report public experimental demonstrations of the findings [10], [21], [22], [23], [24].



Fig. 1. TN3213 models and ground station.

Experimental benchmarking setups for outdoor navigation system based on GNSS and Inertial Navigation System (INS) are rarely deepened, since moving from simulation to real testing is a great challenge even with a reliable simulation environment [25], [26], [27] at disposal for control design [28]. Real world always overcomes many of the ideal assumptions made to design the controllers, and precision may be undermined by odometry complications and unmodeled system nonlinearities. The degree of sophistication of the approach has to be balanced with the resulting performances. With the precise scope, a new experimental test bed and setup have been laid down with the present work.

The main purpose of the present work is the integration and the experimental validation of well-known methodologies developed for automatic navigation of USVs, but in the context of azimuth drives. A follow-the-leader GNC system for azimuthal stern drive vessels is developed by using a LOS control algorithm that allows ensuring yaw-check ability, while a simple supplementary speed-check (+V) feature is adopted to track the velocity of the target along the path [9]. The yaw-check ability concerns the promptness and readiness to adjust and control heading. In these terms, the geometric task to follow a target together with the dynamic task are based on approaches suggested in [18], [19], and [29], but real-time integrated. The adopted motion controller structure is based on [30] and [31] where both stability analysis and synthesis are addressed through linear matrix inequalities (LMIs), which allow accomplishing the control design by solving convex optimization problems. In this work, a more realistic, linearized dynamic model for azimuthal drive surface vessels is deduced from the complete nonlinear modeling framework and experimental testing [5], [32], [33].

The control scheme was validated in two steps, first by using simulations, and then experimentally in a unique outdoor scenario with model-scale vessels with successful results [34], [40]. In that context, a control approach was purposely devised to suit the tug's escorting needs: in fact, the operative profile of the latter concerns long-lasting and routine chases with the continuous demand of tuning heading and speed to track the target vessels, until the rare occurrence of an emergency event. In a realistic scenario, the proposed control system would be beneficial for the tug leader's lucidity and alertness and, thus, risk reduction.

The rest of this article is organized as follows. The experimental setup is described in Section II. The dynamical equation of the follower vessel is presented in Section III. Section IV shows the

proposed follow-the-leader control architecture, including track generation and GNC system. Section V illustrates the proposed experimental setup and manoeuvres carried out to validate the proposed strategy. Finally, Section VI concludes this article.

## II. EXPERIMENTAL SETUP

Two outdoor model-scale 1:33 tugs were considered for the test, as shown in Fig. 1 (for details, see [35]). The two models, named TN3212, are equipped with an inertial measurement unit (IMU) (magnetometers, accelerometers, and gyroscopes) and a GNSS receiver antenna. They are controlled in propeller revolution per minute and azimuth angles through low-level control loops. The GNC modules are realized by using two independent decentralized PCs that close the high-level feedback loop. A radio communication bridge, based on the Zigbee protocol, was designed to broadcast and echo the telemetry information between the two control stations with a wireless serial communication protocol.

A sketch of the overall setup is shown in Fig. 2. Each vessel was equipped with two Arduino Mega 2560 boards, based on an ATmega 8-bit microprocessor (MCU). The hardware architecture was designed to have two separate software layers: one dedicated to processing the control input received from the control station (e.g., the azimuth reference angles and desired propeller speed), while the other was designed to handle the GNSS/INS sensor data. In the following, we will refer to the two MCUs as the main processor (MP) and the navigation processor (NP).

The MP was intended as the local onboard low-level controller. It was equipped with an Xbee asynchronous radio receiver that enables to acquire the reference angle and revolution per minute data. In the meantime, it collects the sensor data from the azimuth motors' encoder and provides the necessary amount of power to the engines managing the actuator low-level control loop. It is also designed as a querier and collector of the sensed telemetries in a full-duplex communication topology between vessels and on-shore stations. The internal clock rate was shaped on the engine shaft revolution frequencies to allow for an effective control. Engine maximum rates are about 3300 r/min. The management of the PWM dc-engine powering in revolution and the helm servo in angle are accomplished through an internal feedback loop.

The NP is directly connected to a geo-referenced GNSS receiver (Ublox Neo-7 m), with an update frequency of 1 Hz, and to an inertial 9-DoF IMU (Adafruit BNO055) with a working

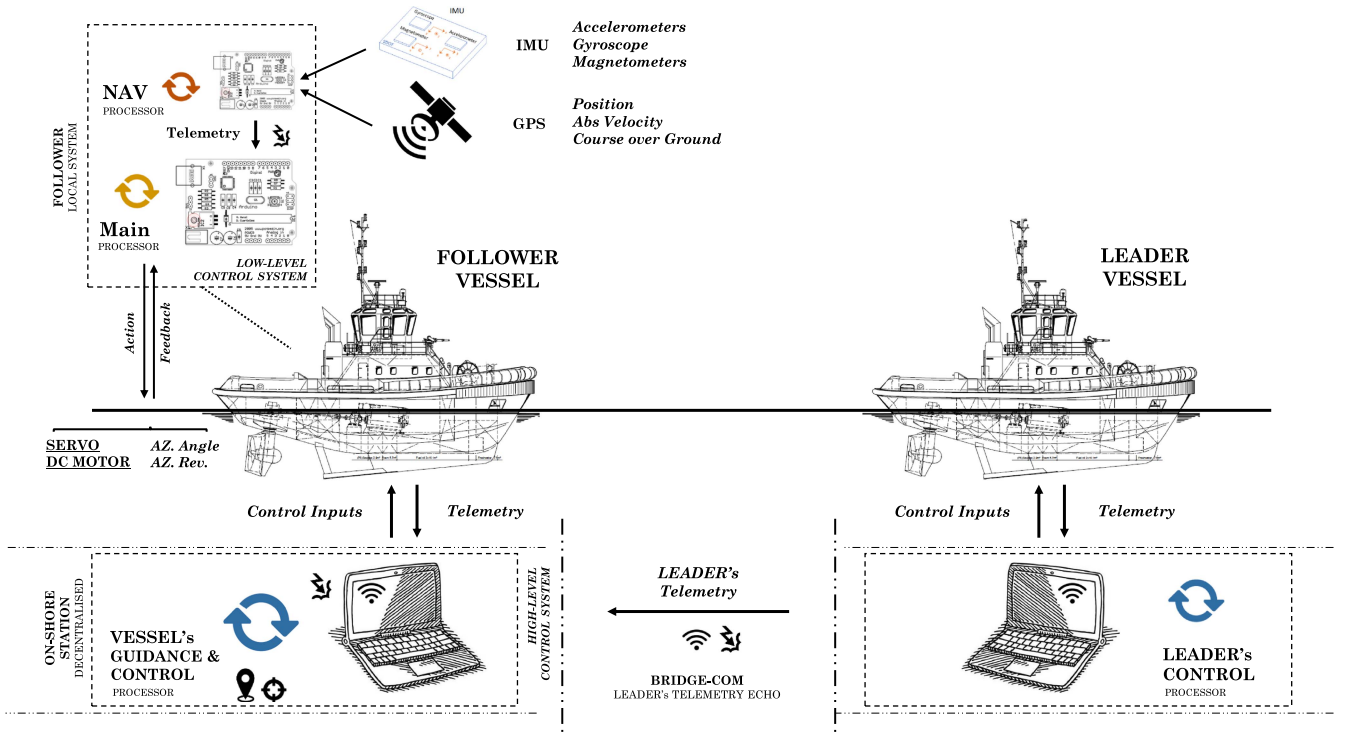


Fig. 2. Experimental setup.

frequency of 100 Hz. It was devised for gathering the onboard navigation instrumentation data at 100-Hz sampling frequency, ready to supply it to the MP at any query, in a leader–follower communication protocol.

Decentralized control was conceived for the on-shore control stations through two independent laptops, connected by means of wireless Xbee asynchronous serial communication to the vessels. At each PC query, the vessel MPs forward the telemetries, thus allowing for the computation of the control inputs. The tasks of track generation and guidance were, thus, remotely processed and overlaid onto the screen in a user interface, while control actions were sent back to the vessels, in this way closing the high-level feedback loop. A high-level control loop at a 10-Hz frequency performs together with the INS refresh, while the GNSS updates run at a rate of 1 Hz.

A second wireless Xbee asynchronous serial cross-communication between the two laptops was set to share relative positioning information, i.e., the bridge communication. The leadership's telemetry was online shared to the trailing vessel using another callback, triggering at each data refresh. In case of delay in refreshing or communicating new data, the tug proceeds with previous information and estimates. The two tugs were conceived completely independent and robust to each other's failure, and in the case of emergency, fully recoverable in real-time manual mode.

### III. STATE EQUATION OF THE FOLLOWER VESSEL

The concept framework of the hydrodynamic modeling of each vessel starts from the 4-DoF extensive manoeuvring modeling and testing campaign of a novel class of azimuth-driven

escort tugs, as shown in [6]. In particular, the complete nonlinear model of 2.5 m called RM2812 [5] was identified and tuned by means of experimental and numerical captive model testing [36], [37], and then validated through a full-scale campaign on a real 32-m length tug [32]. For the present purpose, a 3-DoF linearized model of the tug dynamics is derived around the straight-ahead sailing point at a design speed  $\bar{u}$  with zero drift and zero yaw, and thus well suited for the specific controller design adopted in the present experimental campaign. As a result, the dynamic equation describing the evolution of the vessel is based on the state variables given by  $u$ ,  $v$ , and  $r$  denoting surge speed, sway speed, and yaw rate in a body-fixed frame, respectively;  $\bar{u}$  is the surge speed regarded as linearization point. Reading Newton's laws in the vessel-fixed reference, in a similar fashion to [38], we have

$$(m - X_{\dot{u}}^H) \dot{u} = X_u^H u + 2X_n^{AZ} n + 2X_u^{AZ} u \quad (1a)$$

$$(m - Y_{\dot{v}}^H) \dot{v} - Y_r^H \dot{r} + m(\bar{u}r + x_G \dot{r}) = Y_v^H v + Y_r^H r + 2Y_{\delta}^{AZ} \delta + 2Y_v^{AZ} v + 2Y_r^{AZ} r \quad (1b)$$

$$(I_{zz} - N_{\dot{r}}^H) \dot{r} + (m x_G - N_v^H) \dot{v} + m x_G \bar{u} r = N_v^H v + N_r^H r + 2x_{AZ} Y_{\delta}^{AZ} \delta + 2x_{AZ} Y_v^{AZ} v + 2x_{AZ} Y_r^{AZ} r \quad (1c)$$

$$\dot{\psi} = r \quad (1d)$$

where all the parameters in (1a)–(1c) refer to the vessel's hydrodynamics and Coriolis-centripetal Jacobian terms (see Appendix A), according to which the subscript denotes the derivation variable and the apex  $H$  and  $AZ$  refer to the hull and azimuth-drive contributions, respectively;  $m$  and  $I_{zz}$  are



the mass and yaw inertia, respectively;  $x_G$  and  $x_{AZ}$  account for the longitudinal position of the centre of gravity and of the azimuths, respectively. Second, (1d) is just the kinematic relation between yaw and yaw rate. In addition, we need to account for the azimuthal actuators by means of the first-order equations

$$\dot{n} = \frac{1}{\tau_{AZ}^n} (n_{\text{set}} - n) \quad (2a)$$

$$\dot{\delta} = \frac{1}{\tau_{AZ}^\delta} (\delta_{\text{set}} - \delta) \quad (2b)$$

with the additional state variables  $n$  (revolution rate) and  $\delta$  (azimuth angle) and their corresponding setpoints  $n_{\text{set}}$  and  $\delta_{\text{set}}$ ;  $\tau_{AZ}^n > 0$  and  $\tau_{AZ}^\delta > 0$  are time constants.

The azimuthal control action plays actively a longitudinal force  $X_n^{AZ}$  depending on revolutions and a lateral force  $Y_\delta^{AZ}$  together with a yaw moment  $N_\delta^{AZ}$  as a function of the helm angle. The passive action instead counts the damping contributions relative to the propeller loss of thrust with speed  $X_u^{AZ}$ , the lateral force to drift  $Y_v^{AZ}$ , and the resistance to rotation due to their astern positioning, i.e.,  $N_r^{AZ}$ .

In the linearized context (small variations of the variables), propeller revolution and azimuth-angle effects play separated roles in surge and sway–yaw dynamics, de facto uncoupling completely the two dynamics. Moreover, port-side and starboard-side azimuthal contributions become identical, leading to a factor 1 or 2 in case they are used individually or together. Thus, the state and input vectors of the overall system, including the propeller revolutions and azimuthal angle actuators, are given by  $\mathbf{x}^p = \mathbf{x} - \mathbf{x}_0 = [u^p, v, r, \psi, n^p, \delta]^T \in \mathbb{R}^6$  and  $\mathbf{u} = [n_{\text{set}}, \delta_{\text{set}}]^T \in \mathbb{R}^2$  with state equations from (1) and (2) as follows, once provided the straight sailing linearization point  $\mathbf{x}_0 = [\bar{u}, 0, 0, 0, \bar{n}, 0]^T \in \mathbb{R}^6$ :

$$\dot{\mathbf{x}}^p = \mathbf{A}\mathbf{x}^p + \mathbf{B}\mathbf{u} \quad (3)$$

where  $\mathbf{A} \in \mathbb{R}^{6 \times 6}$  having all zero elements except

$$\begin{aligned} A_{1,1} &= (X_u^H + X_u^{AZ})/(m - X_u^H) & A_{2,2} &= \bar{Y}_v & A_{2,3} &= \bar{Y}_r \\ A_{3,2} &= \bar{N}_v/\bar{M}_r & A_{3,3} &= \bar{N}_r/\bar{M}_r \\ A_{4,3} &= 1 \end{aligned}$$

with

$$\begin{aligned} \bar{N}_v &= (Y_v^H + 2Y_v^{AZ})(N_v^H - m x_G)/(m - Y_v^H) \\ &\quad + N_v^H + 2x^{AZ} Y_v^{AZ} \\ \bar{M}_r &= I_{zz} - N_r^H - (Y_r^H - m x_G)(N_v^H - m x_G)/(m - Y_v^H) \\ \bar{Y}_v &= (Y_v^H + 2Y_v^{AZ})/(m - Y_v^H) \\ &\quad + (Y_r^H - m x_G)/(m - Y_v^H)(\bar{N}_v/\bar{M}_r) \\ \bar{N}_r &= (Y_r^H + 2Y_r^{AZ} - m\bar{u})(N_v^H - m x_G)/(m - Y_v^H) \\ &\quad + N_r^H + 2x^{AZ} Y_r^{AZ} - m x_G \bar{u} \\ \bar{Y}_r &= (Y_r^H + 2Y_r^{AZ} - m\bar{u})/(m - Y_v^H) \\ &\quad + (Y_r^H - m x_G)/(m - Y_v^H)(\bar{N}_r/\bar{M}_r) \end{aligned}$$

and parameters of the actuators given by

$$\begin{aligned} A_{1,5} &= 2X_n^{AZ}/(m - X_u^H) & A_{2,6} &= \bar{Y}_\delta & A_{3,6} &= \bar{N}_\delta/\bar{M}_r \\ A_{5,5} &= -1/\tau_{AZ}^n & A_{6,6} &= -1/\tau_{AZ}^\delta \end{aligned}$$

with

$$\begin{aligned} \bar{N}_\delta &= 2Y_\delta^{AZ}(x_{AZ} + (N_v^H - m x_G)/(m - Y_v^H)) \\ \bar{Y}_\delta &= 2((Y_r^H - m x_G)/(m - Y_v^H)\bar{N}_\delta/\bar{M}_r \\ &\quad + Y_\delta^{AZ}/(m - Y_v^H)). \end{aligned}$$

The matrix  $\mathbf{B} \in \mathbb{R}^{6 \times 2}$  has all zero elements except

$$B_{5,1} = 1/\tau_{AZ}^n \quad B_{6,2} = 1/\tau_{AZ}^\delta.$$

From now on, we refer to (3) as the ‘‘dynamics of the follower.’’

#### IV. SYSTEM ARCHITECTURE

The controller framework is based on the cooperation of both guidance and motion control systems. Indeed, the proposed approach relies on the closed-loop controllers based on two levels: 1) the guidance system that receives input from the leader and generates setpoints to the lower level, and 2) the motion control that closes the loop on the follower. In detail, the workflow diagram, sketched in Fig. 3, represents the proposed follow-the-leader GNC system. From top to bottom, the signal flows and blocks are described as follows:

- 1) *leader module*—broadcasts of GPS position to the ground station;
- 2) *track generation and guidance module*—green box, which collects, records, elaborates leader’s trajectory, processes the relative position errors, and translates them into heading and speed setpoints;
- 3) *navigation and control module*—red box, which provides an estimate of the state variables (using a Kalman filter) and includes heading and speed pilots that turn the heading and speed errors into the lever positions (azimuth angle and shaft-line revolution) of the actuators;
- 4) *follower module* actuates the control setpoints internally and feeds back the actual state, thanks to sensors.

The main idea is to maintain two independent controllers for autopilot and speed controller, namely, a sort of integrated ‘‘LOS+V’’ approach. The first one accounts for (1c), while the second deals with (1a). These two systems operate in a parallel mode without affecting each other performances. The proposed approach is well suited for both analysis and synthesis based on linear-coupled equations. In particular, the entire state matrix was considered in the process, which, therefore, also includes (1b) relating the two controllers. A simplified model is adopted to take into account for dynamics that could affect the controller performances, without overcomplicating the controller structure.

Fig. 4 sketches the details of the problem geometry, according to the relative positioning of leader and follower denoted with  $\mathbf{x}_\ell := [x_\ell, y_\ell]$  and  $\mathbf{x}_f := [x_f, y_f]$ , respectively.  $\boldsymbol{\pi}_\ell(t)$  represents the filtered positions of the leader’s position. A complementary LOS+V algorithm is used to supply suitable heading and speed

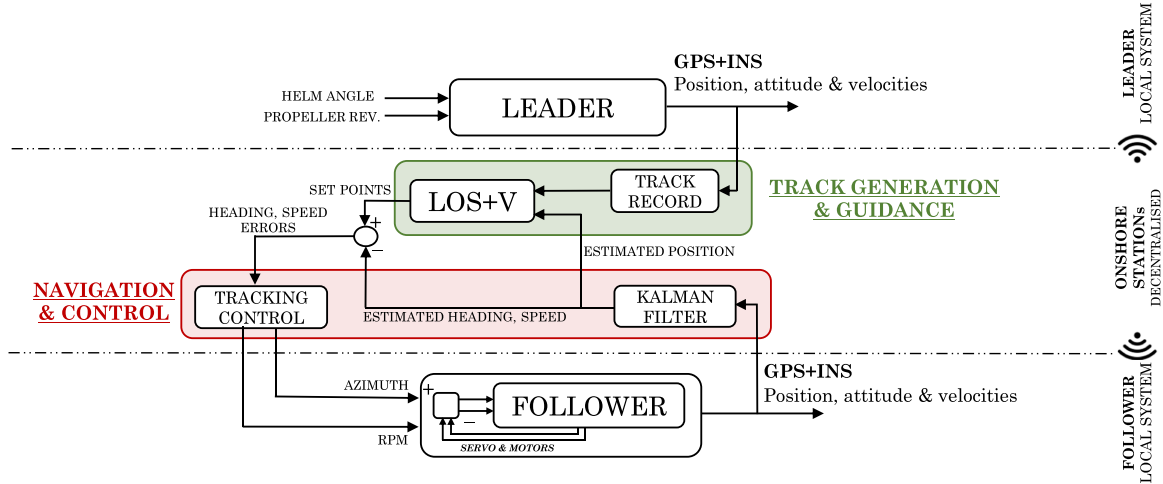
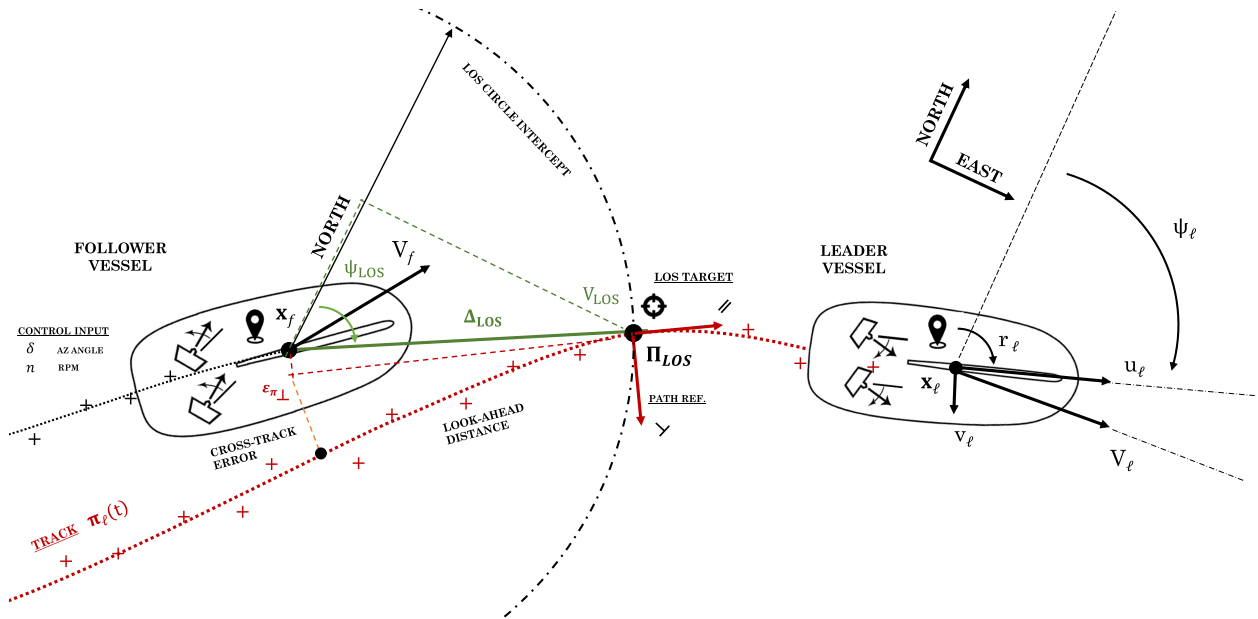


Fig. 3. Follow-the-leader control architecture.

Fig. 4. Geometrical overview of the algorithm LOS+V, where  $\psi_l$ ,  $r_l$ ,  $u_l$ ,  $v_l$ , and  $V_l$  denote the heading, yaw rate, surge velocity, sway velocity, and speed of the leader, respectively. The  $f$  subscript denotes the follower one. The latter control action is based onto the setting of the azimuth angle  $\delta$  and propeller revolutions  $n$ .

setpoints [18], [19], whose aim is to ensure a precise tracking of the desired path taken just equal to  $\pi_\ell(t)$ , which will be obtained by filtering the GPS measurements by a Savitzky–Golay filter.

#### A. Kalman Filtering

The follower's position  $x_f$  can be assessed by integrating the rotated vessel-fixed velocities w.r.t. the Earth-fixed reference, which are north-east aligned. As a consequence, the time derivatives of the position are given by

$$\dot{x}_f = (\bar{u} + u^p) \cos \psi - v \sin \psi \quad (4a)$$

$$\dot{y}_f = (\bar{u} + u^p) \sin \psi + v \cos \psi \quad (4b)$$

which augment the dynamics of the follower. Thus, an EKF can be designed by combining (3) and (4) linearized around the last

estimated state and by using the available measurements given as follows:

- 1) accelerometer linear velocities, gyro angular velocity, and magnetometer heading reference (from the vessel-fixed IMU);
- 2) follower's position in Earth-fixed coordinates (from the GPS);
- 3) propeller revolution and azimuth angle (from the low-level internal control loop).

The EKF turns out to be only a predictor as it provides a dead-reckoning estimation when the system with the available measurements is not fully observable. The measurement equations are adapted online depending on the available measurements at each sampling time, according to the different sensor rates. In the following, we will denote by  $\hat{\pi}_f(t)$  the estimate of the follower position at time  $t \geq 0$ .



Fig. 5. Experimental model tests: leader (orange) and follower (blue).

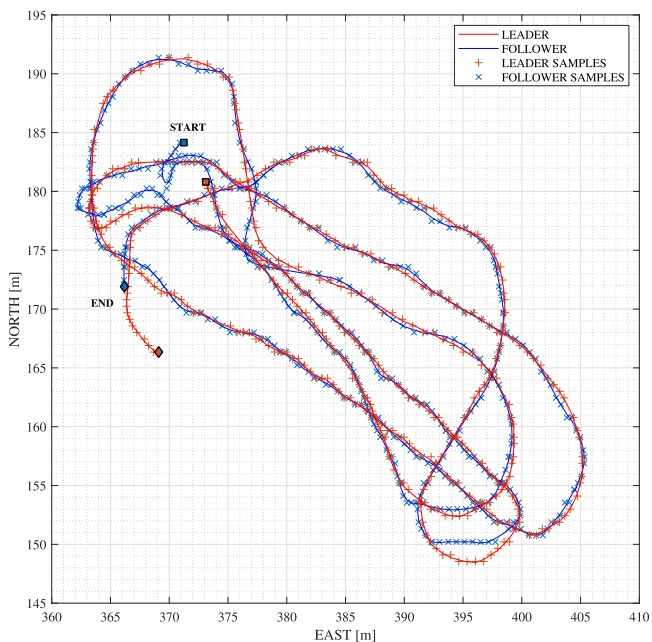


Fig. 6. Experimental model testing (wide-runs): trajectories.

### B. Track Generation

The leader's trajectory is collected and used to get a smooth trajectory  $\pi_\ell(t) = [x_\ell(t), y_\ell(t)]$ , where  $x_\ell(t)$  and  $y_\ell(t)$  are the coordinates in the north-east frame and subscript  $\ell$  refers to the leader (see Fig. 4), to be fed to the guidance and control modules. In more detail, a Savitzky–Golay filter was chosen to process the leader's raw GPS data, thus making available at each time  $t$  two sets of pairs  $\{[x_\ell(t_i), y_\ell(t_i)], i = 1, \dots, m\}$  and  $\{[\dot{x}_\ell(t_i), \dot{y}_\ell(t_i)], i = 1, \dots, m\}$  with  $t_{i+1} > t_i, i = 1, \dots, m$

and  $t_1 = t$ . In practice, the leader's trajectory and velocity are fitted over a moving window of length  $m$  at each time sample  $t_i$  with a low-degree polynomial, distinct in  $x, y$ . A third-degree polynomial in the Savitzky–Golay filter was selected based on the vessel response readiness to cut higher frequencies not related to relevant ship motions. The smoothness of the trajectory to be followed combined with the regularity of its time derivative is beneficial for path and setpoint generation.

### C. LOS+V Algorithm

The guidance algorithm generates the angle/speed setpoints  $\psi_{\text{LOS}}(t)$  and  $V_{\text{LOS}}(t)$  for the control system of the follower to succeed in the pursuit.

Using the current estimate of follower position and filtered trajectory and speed of the leader, the LOS intercept can be found by drawing the look-ahead circle with a given radius  $\Delta_{\text{LOS}} = nL$ , where  $L$  is the vessel length and  $n$  is the number of lengths to choose. This is obtained by solving the system of equations in  $x$  and  $y$  given by

$$\begin{cases} \min_{i=1, \dots, m} (\| [x_\ell(t_i), y_\ell(t_i)] - \hat{\pi}_f(t_i) \| - \Delta_{\text{LOS}})^2 \\ [\dot{x}_\ell(t_i), \dot{y}_\ell(t_i)] \cdot ([x_\ell(t_i), y_\ell(t_i)] - \hat{\pi}_f(t_i)) > 0 \end{cases} \quad (5)$$

where the inequality constraint guarantees an advance speed contribution in the direction of the target displacement along the path. In the case of two regular intersections, the scalar product excludes the rear one; in the case of several solutions, the nearest one to the leader in terms of curvilinear abscissa is selected. This corresponds to the newest obtained intersection in time. If we denote the solution of (5) by

$$\mathbf{\Pi}_{\text{LOS}}(t) = [x_{\text{LOS}}(t), y_{\text{LOS}}(t)]^\top$$



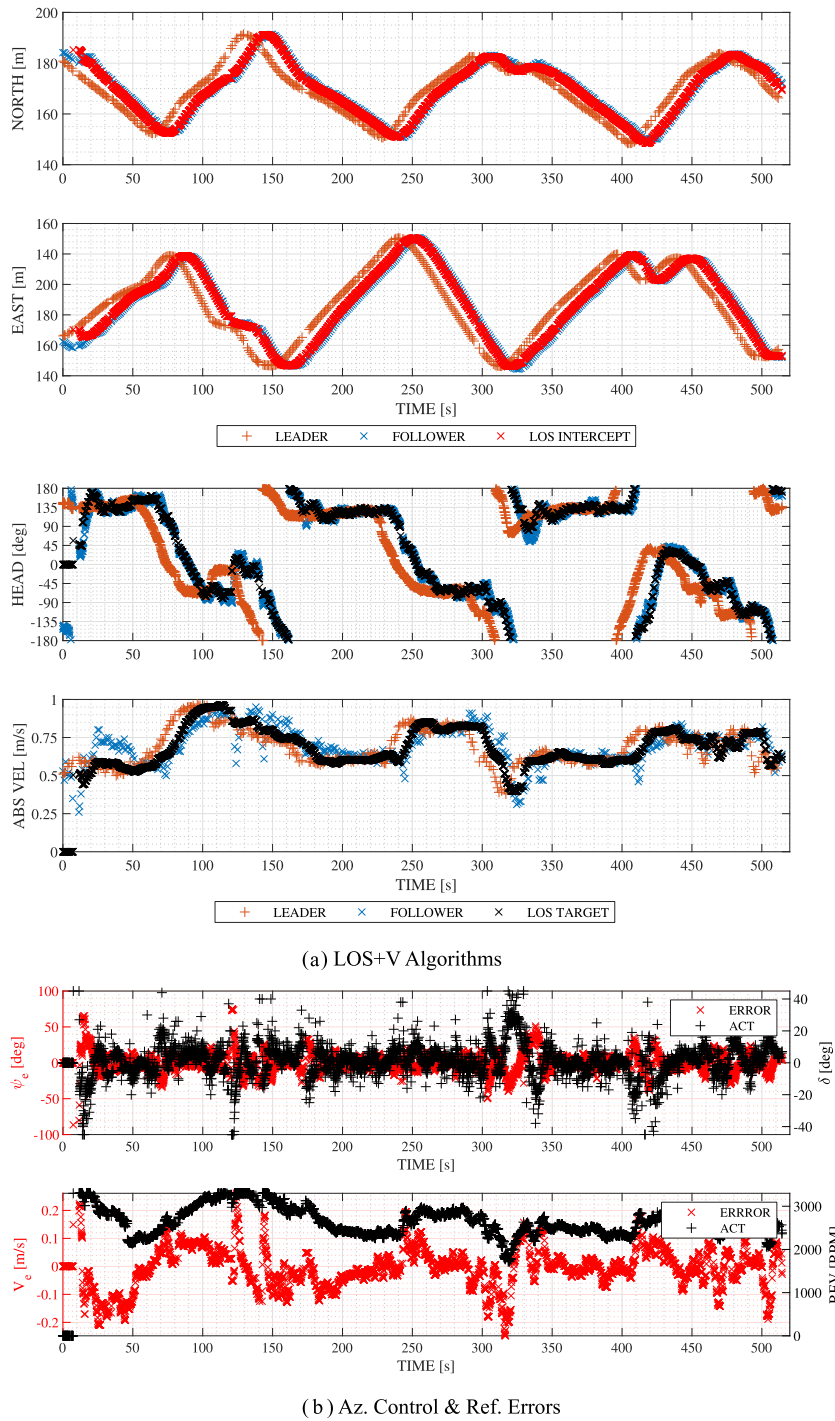


Fig. 7. Experimental model testing (wide-runs): controller setpoints and actuation. (a) LOS+V algorithms. (b) Az. control and ref. errors.

it is straightforward to obtain the LOS intercept angle and speed as follows:

$$\psi_{\text{LOS}}(t) := \arctan \left( \frac{y_{\text{LOS}}(t) - \hat{y}_f(t)}{x_{\text{LOS}}(t) - \hat{x}_f(t)} \right)$$

$$V_{\text{LOS}}(t) := \|\dot{\pi}_\ell(x_{\text{LOS}}(t), y_{\text{LOS}}(t))\|$$

to be fed to the tracking controllers. The tracking control aims at performing the follow-the-leader task with an appropriate

steering at a speed  $V_f(t) := (\dot{x}_{\text{LOS}}(t)^2 + \dot{y}_{\text{LOS}}(t)^2)^{1/2}$  as much as possible close to the intercept speed  $V_{\text{LOS}}(t)$  and along the course with the yaw angle  $\psi_{\text{LOS}}(t)$  in such a way as to safely follow the path traced by the leader vessel.

#### D. Tracking Controllers

The maritime practice fosters the simplicity and robustness of control algorithms [39]. PID controllers allow to successfully

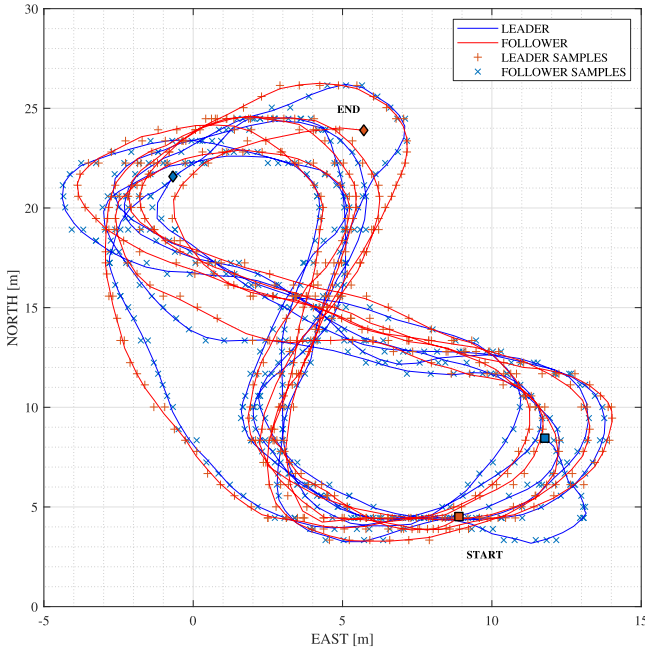


Fig. 8. Experimental model testing (8-runs): trajectories.

deal with most of the mechanical systems, which are often reducible to second-order dynamics. The control is obtained by evaluating the actual error of the desired quantity to be controlled and by devising a suitable control action. Three coefficients are adopted for the tuning, i.e., the proportional  $k_p$ , integral  $k_i$ , and derivative  $k_d$  parameters. The transfer function to be dealt is

$$G(s) = k_p + k_i \frac{1}{s} + k_d s.$$

Thus, we consider the speed and heading errors given by  $e_u(t) := u_d(t) - \hat{u}^p(t)$  and  $e_\psi(t) := \psi_d(t) - \hat{\psi}(t)$ , where  $\hat{u}^p(t)$  and  $\hat{\psi}(t)$  are the estimates of  $u^p(t)$  and  $\psi(t)$ , respectively. In particular, the latter to be fed are equal to  $V_{LOS}(t)$  and  $\psi_{LOS}(t)$ , respectively. Thus, the input setpoints to the local controller are given by

$$n_{\text{set}}(t) = k_p^u e_u(t) + k_i^u \int_0^t e_u(\tau) d\tau + k_d^u \dot{e}_u(t) \quad (6a)$$

$$\delta_{\text{set}}(t) = k_p^\psi e_\psi(t) + k_i^\psi \int_0^t e_\psi(\tau) d\tau + k_d^\psi \dot{e}_\psi(t) \quad (6b)$$

where  $k_p^u, k_i^u, k_d^u$  and  $k_p^\psi, k_i^\psi, k_d^\psi$  are the sets of control parameters for speed and heading, respectively.

To address the control design in a state-space representation, let us introduce the two new state variables

$$\epsilon_u(t) := \epsilon_u(0) + \int_0^t e_u(\tau) d\tau$$

and

$$\epsilon_\psi(t) := \epsilon_\psi(0) + \int_0^t e_\psi(\tau) d\tau.$$

Thus, the augmented linear system is described by the set of the tug's dynamics (including actuators) (3) and the controller dynamics (6). We define the extended state vector  $x_e :=$

$[x^p, \epsilon_u, \epsilon_\psi]^T$  and obtain the state equation

$$\dot{x}_e = A_e x_e + B_e u$$

where  $A_e$  and  $B_e$  are the augmented system matrices, see Appendix B.

Using the system description given previously, we set the state feedback control action  $u = -K_e x_e + E_e u_d$ , where the matrices  $K_e$  and  $E_e$  include PID parameters and  $u_d := [u_d, \psi_d]^T$ . Thus, we obtain

$$\dot{x}_e = (A_e - B_e K_e) x_e + B_e E_e u_d.$$

The controller synthesis has been performed by using the Lyapunov-based approach reported in [30], to which the interested reader is referred to. In particular, LMI-based techniques enable to compute the design parameters by means of convex optimization algorithms for selecting the closed-loop matrix  $A_e - B_e K_e$  with the Lyapunov function  $V(x_e) = x_e^T Q x_e$ ,  $Q = Q^T > 0$ . Thus, the gain  $K_e$  was found by solving LMI program

$$\begin{aligned} & \min_{P, Y} \text{tr}(P) \\ & \text{s.t. } P > 0 \\ & \quad P A_e^T - Y^T B_e^T + A_e P - B_e Y < 0 \end{aligned} \quad (7)$$

where  $P := Q^{-1}$ , i.e.,  $K_e = Y P^{-1}$ .

## V. EXPERIMENTAL VALIDATION

To assess the performance of the proposed approach, an experimental campaign is carried out at the ResearchLab on Autonomous Shipping of the Delft University of Technology, 3mE Lake facility. Two 1:33 TN3212 model-scale azimuthal stern drive tugs (see Fig. 1) were instrumented for outdoor remote-controlled navigation (see Fig. 5). The TN3212 manoeuvring linear coefficients were deduced and calibrated according to a customary identification in the first steps of the experimental activities, based on [5] and [34]. The orange tug was chosen as the leader upon manual or automatic sailing with varying course and speed, while the blue tug was the follower (see Fig. 5).

Manual control through a joystick was provided to start navigation and backup in the case of failures to recover the vessels. The follow-the-leader strategy was switched ON, once the vessels were initialized at speed. The integral part was smoothly activated to avoid unstable behaviors due to the controller initial transients. Azimuthals were helmed parallel and tuned synchronously in engine revolutions. We chose a maximum angle of about  $45^\circ$ , while max engine revolutions were about 3300 r/min. Experiments have been conducted with a sailing speed such as in full-scale correspond to a range of 6–12 kn.

The proposed validation manoeuvring scenario concerns two different runs. The first one consists of a smooth, wide manoeuvring pattern to check the ability of the algorithms in suiting the smaller manoeuvring assumption; it will be called *wide-runs*. Instead, the second one further pushes the algorithms by engaging narrower turnings in an eight-shaped pattern, thus called *8-runs*. In both cases, the leader vessel was sailed manually, while the follower engaged the pursuit.

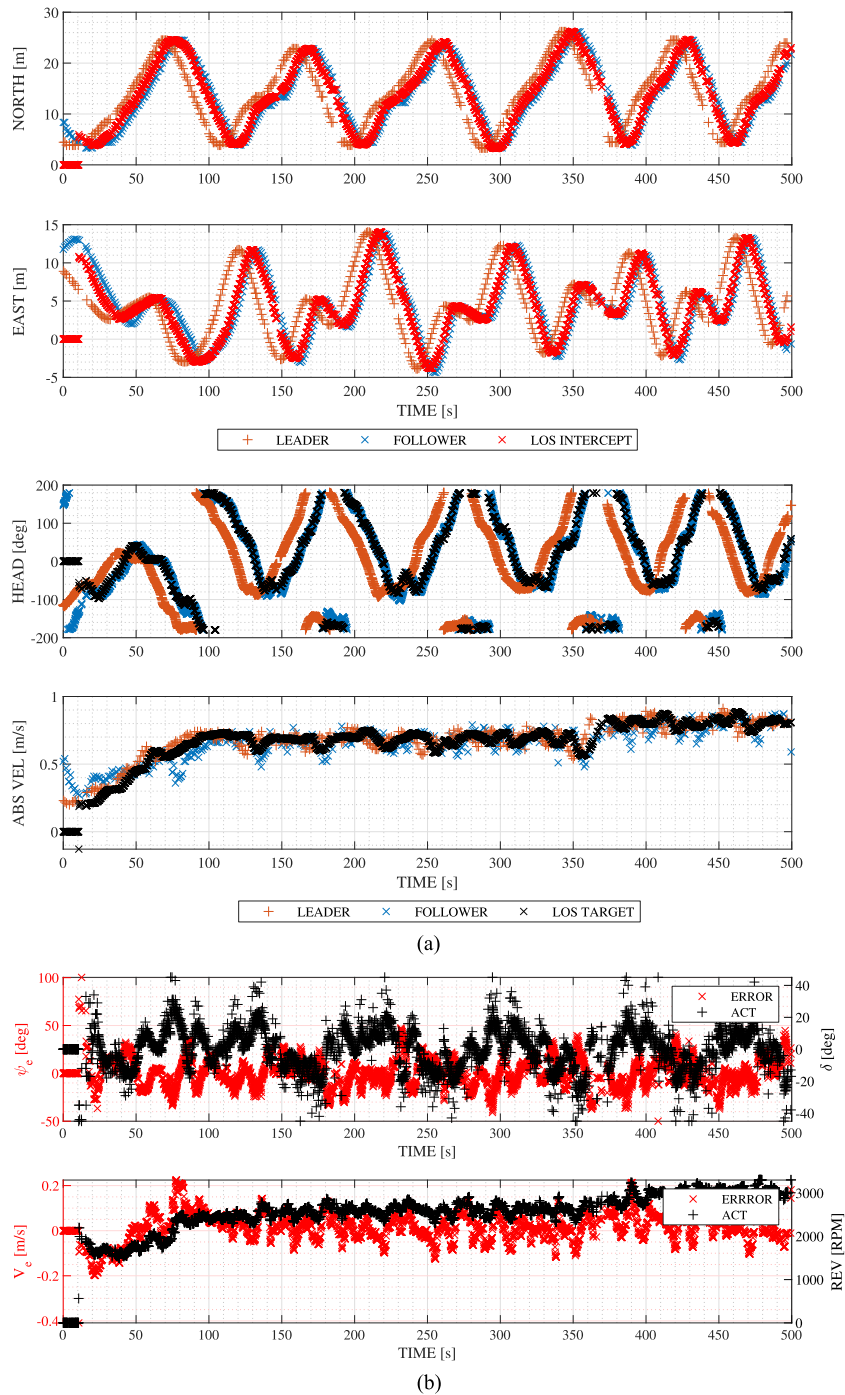


Fig. 9. Experimental model testing (8-Runs): controller setpoints and actuation. (a) LOS+V algorithms. (b) Az. control and ref. errors.

The convoy trajectories are depicted in Figs. 6 and 8. The orange tug is the leader (orange lines and markers), while the blue one follows (blue lines and markers). Crossed markers refer to the raw measurements of positions, processed then by the track generation algorithm, which results in solid smoothing lines. The squared and diamond markers point the start and the end of the tests, respectively. The precision in position is immediately geometrically noticeable by keeping a bounded cross-track error within 0.3 m on average: the ensemble of trajectories satisfactorily tightens in a narrowband, especially

keeping in mind the normal GPS limitations at very small scales. The presented complete test successfully lasted more than 10 min without human intervention.

The LOS algorithm intercept coordinates (north and east) and its corresponding heading and speed guidance setpoints are overlaid with the actual quantities in Figs. 7(a) and 9(a) time series. Controllers are started as soon as the track generation algorithm is prefilled and initialized within the first 10 s. Once the target is engaged, control setpoints and actual quantities almost result in a time-delayed version of the leader state asymptotically. In

fact, the follower's series (blue marks) converge in position to the LOS target intercept values at algorithm engagement (red marks), while reacting at the leader's heading and speed variations (see actual values—blue marks and overlapping to setpoints—black marks). This illustrates the algorithm ability in retracing the leader's path and speed, always keeping within its wake.

Figs. 7(b) and 9(b) show the vessel control sequences, i.e., helm azimuth angles and propeller revolutions. Error time series in heading and speed (red, left axis) are compared with the actual azimuth control actions in angles and revolutions (black, right axis). This representation is used to emphasize the closed-loop response of the system. The initial transient phase (5–10 s) in the activation of controllers is rapidly handled with a satisfactory convergent response. Then, in detail, the two controllers perform quite well by tracking the variations of the setpoints. On the one hand, faster and harsher responses are handled by the heading-check controller due to the fast response to the action of azimuthal helming. On the other hand, intentionally softer raise and descent in speed occur due to the slower dynamics in the surge speed. As a consequence, both heading and speed errors quickly approach zero.

The yaw-check and speed-check ability of the LOS+V algorithm ensure a satisfactory tracking performance. When turning, the speed loss and the heading error steps are handled by the controllers smoothly. Thus, the manoeuvring nonlinearities do not undermine the effectiveness of the PID control in the case of narrow turning, as it results from using the linearized model and the LMI-based controller synthesis.

## VI. CONCLUSION

Design and testing of a follow-the-leader approach have been investigated in the context of the increasingly growing interest in the control of autonomous vessels with a potentially massive impact on the shipping industry. Synchronization among vessels of the same convoy, real-time exchange of information to exploit the optimal sailing path in crowded and narrow environments would indeed open the possibility to optimize the logistic framework by minimizing maneuvering delays with a substantial return in the future evolution of the maritime transport. On the one hand, the subject matter deeply pervades many civil applications, such as, for instance, in restricted waters and inland navigation, platooning of autonomous vessels and barges along inland corridors, and especially the deployment of autonomous escorting routes from blue waters fairways to the final berths. On the other hand, naval research will be permeated by topics, such as swarming, platooning, surveying/reconnaissance, and cooperative formation of unmanned vehicles. In this context, an original follow-the-leader control scheme for azimuth-drive surface vessels has been investigated, practically designed, and experimentally validated in a novel outdoor model-scale campaign. This originally “closes the loop” of an innovative and proactive framework that fills the gap between theory control and real-world application.

The experiments satisfactorily demonstrate the effectiveness and robustness of the proposed approach in all the complications

of an experimental setup, which involve real-world non-scalable instrumentation precision and accuracy, wireless serial transmission delays, and lost ticks of two contemporary hardware and software independent vessels, and multimachine clock synchronization issues. The algorithms are simple and easily implementable on digital microprocessors with a wireless XBee asynchronous serial communication in the high-level feedback loop at a sampling frequency of about 10 Hz.

Future insights will be carried out by accounting for environmental disturbances within the considered modeling framework in spite of nonideal testing conditions. In addition, an in-depth check of the whole process will be investigated by means of a stability analysis of the closed-loop system. Furthermore, in order to demonstrate the experienced results, robustness requirements in the controller design will be addressed. Moreover, since increasing the number of the convoy vessels would exponentially raise the complexity of the communication network topology, a new communication system will be considered, where every ship would be able to directly be connected to all the other vessels of the same platoon as to allow to share their states data in real time. This demands investigations of new communication technologies based on Transmission Control Protocol and User Datagram Protocol, such as the 5G data network.

In conclusion, the small-scale complications given by the accuracy of the GPS system (which easily could be improved by means of dGPS techniques) and the adoption of simple and almost straight-scalable navigation and communication equipments satisfactorily foster promising results for near-future real full-scale applications, such as those concerning escorting.

## APPENDIX A SYSTEM JACOBIANS

### A. Hull Forces

Given the straight sailing design speed  $\bar{u}$ , the Jacobians of the hydrodynamic forces are evaluated by the partial derivative of the forces and moments with respect to velocities (damping terms) and accelerations (added mass terms) in the vessel reference as follows:

$$\begin{aligned} X_u^H &= - \left. \frac{dR_T}{du} \right|_{u=\bar{u}} \\ Y_v^H &= \left. \frac{\partial Y}{\partial v} \right|_{[u=\bar{u}, v=0, r=0]} & Y_r^H &= \left. \frac{\partial Y}{\partial r} \right|_{[u=\bar{u}, v=0, r=0]} \\ N_v^H &= \left. \frac{\partial N}{\partial v} \right|_{[u=\bar{u}, v=0, r=0]} & N_r^H &= \left. \frac{\partial N}{\partial r} \right|_{[u=\bar{u}, v=0, r=0]} \\ Y_{\dot{v}}^H &= \left. \frac{\partial Y}{\partial \dot{v}} \right|_{\dot{v}=0} & Y_{\dot{r}}^H &= \left. \frac{\partial Y}{\partial \dot{r}} \right|_{\dot{r}=0} \\ N_{\dot{v}}^H &= \left. \frac{\partial N}{\partial \dot{v}} \right|_{\dot{v}=0} & N_{\dot{r}}^H &= \left. \frac{\partial N}{\partial \dot{r}} \right|_{\dot{r}=0} \end{aligned}$$

where  $X$ ,  $Y$ , and  $N$  the longitudinal force, the lateral force, and the yaw moment with respect to midship, respectively;  $R_T$  is the vessel resistance to surge.



### B. Azimuthal Forces

Given the design revolution setpoint  $n_0$  of the propeller at zero azimuth angle, the Jacobians with respect to their variations is considered, given  $\epsilon_e$  the effective advance angle of propeller, and  $\delta_e$  the effective angle of attack of the azimuth with respect to the flow at a speed  $\bar{u}$

$$X_u^{AZ} = \frac{\partial X^{AZ}}{\partial \epsilon_e} \frac{\partial \epsilon_e}{\partial u} \Big|_{[u=\bar{u}, n=n_0, \delta=0]}$$

$$X_n^{AZ} = \frac{\partial X^{AZ}}{\partial \epsilon_e} \frac{\partial \epsilon_e}{\partial n} \Big|_{[u=\bar{u}, n=n_0, \delta=0]}$$

$$Y_n^{AZ} = 0 \quad Y_v^{AZ} = a_H \frac{\partial Y^{AZ}}{\partial \delta_e} \frac{\partial \delta_e}{\partial v} \Big|_{[u=\bar{u}, n=n_0, \delta=0]}$$

$$Y_r^{AZ} = a_H \frac{\partial Y^{AZ}}{\partial \delta_e} \frac{\partial \delta_e}{\partial r} \Big|_{[u=\bar{u}, n=n_0, \delta=0]}$$

$$Y_\delta^{AZ} = a_H \frac{\partial Y^{AZ}}{\partial \delta_e} \Big|_{[u=\bar{u}, n=n_0, \delta=0]}$$

$$N_v^{AZ} = (x_{AZ} + a_H x_{aH}) Y_v^{AZ}$$

$$N_r^{AZ} = (x_{AZ} + a_H x_{aH}) Y_r^{AZ}$$

$$N_\delta^{AZ} = (x_{AZ} + a_H x_{aH}) Y_\delta^{AZ}$$

where  $x_{AZ}$  is the longitudinal geometrical position of the azimuthals with respect to midship;  $a_H$  and  $x_{aH}$  are the amplification factors due to the hull-azimuth interaction and its longitudinal application point, respectively.

#### APPENDIX B AUGMENTED LINEAR MODEL

Given the augmented state  $\mathbf{x}_e := [u, v, r, \psi, n, \delta, \epsilon_u, \epsilon_\psi]^\top$  and according to the state feedback control action with setpoint  $\mathbf{u}_d := [u_d, \psi_d]^\top$

$$\dot{\mathbf{x}}_e = \mathbf{A}_e \mathbf{x}_e + \mathbf{B}_e \mathbf{u}$$

$$\mathbf{u} = -\mathbf{K}_e \mathbf{x}_e + \mathbf{E}_e \mathbf{u}_d$$

it is straightforward to verify that

$$\mathbf{A}_e = \left( \begin{array}{cccccc|c} A & & & & & & 0_{6 \times 2} \\ -1 & 0 & 0 & 0 & 0 & 0 & \\ 0 & 0 & 0 & -1 & 0 & 0 & 0_{2 \times 2} \end{array} \right)$$

and

$$\mathbf{B}_e = \left( \begin{array}{c} B \\ 0_{2 \times 2} \end{array} \right).$$

In addition,  $\mathbf{K}_e \in \mathbb{R}^{2 \times 8}$  has all zero elements except

$$K_{e1,1} = k_p^u + k_d^u A_{e1,1} \quad K_{e1,5} = k_d^u A_{e1,5}$$

$$K_{e1,7} = -k_i^u \quad K_{e2,2} = -k_p^v \quad K_{e2,3} = +k_d^v$$

$$K_{e2,4} = +k_p^\psi A_{e4,3} \quad K_{e2,6} = -k_p^\delta \quad K_{e2,8} = -k_i^\psi.$$

Finally, we have  $\mathbf{E}_e \in \mathbb{R}^{8 \times 2}$  with all zero elements except

$$E_{e5,1} = k_p^u \quad E_{e7,1} = 1 \quad E_{e6,2} = k_p^\psi \quad E_{e8,2} = 1.$$

#### REFERENCES

- [1] C. Liu, J. Liu, X. Zhou, Z. Zhao, C. Wan, and Z. Liu, "AIS data-driven approach to estimate navigable capacity of busy waterways focusing on ships entering and leaving port," *Ocean Eng.*, vol. 218, 2020, Art. no. 108215.
- [2] L. Chen, A. Haseltalab, V. Garofano, and R. R. Negenborn, "Eco-VTF: Fuel-efficient vessel train formations for all-electric autonomous ships," in *Proc. 18th Eur. Control Conf.*, 2019, pp. 2543–2550.
- [3] K. Wróbel, M. Gil, and J. Montewka, "Identifying research directions of a remotely-controlled merchant ship by revisiting her system-theoretic safety control structure," *Saf. Sci.*, vol. 129, 2020, Art. no. 104797.
- [4] C. Liu, J. Liu, X. Zhou, Z. Zhao, C. Wan, and Z. Liu, "AIS data-driven approach to estimate navigable capacity of busy waterways focusing on ships entering and leaving port," *Ocean Eng.*, vol. 218, 2020, Art. no. 108215.
- [5] B. Piaggio, M. Viviani, M. Martelli, and M. Figari, "Z-drive escort tug manoeuvrability model and simulation," *Ocean Eng.*, vol. 191, 2019, Art. no. 106461.
- [6] M. Figari, L. Martinelli, B. Piaggio, L. Enoizi, M. Viviani, and D. Villa, "An all-round design-to-simulation approach of a new z-drive escort tug class," *J. Offshore Mechanics Arctic Eng.*, vol. 142, no. 3, 2020, Art. no. 031107.
- [7] M. Schiaretto, L. Chen, and R. R. Negenborn, "Survey on autonomous surface vessels: Part I - A new detailed definition of autonomy levels," in *Proc. Int. Conf. Comput. Logistics*, 2017, pp. 219–233.
- [8] M. Schiaretto, L. Chen, and R. R. Negenborn, "Survey on autonomous surface vessels: Part II - Categorization of 60 prototypes and future applications," in *Proc. Int. Conf. Comput. Logistics*, 2017, pp. 234–252.
- [9] T. Fossen, *Marine Control Systems: Guidance, Navigation and Control of Ships, Rigs and Underwater Vehicles*. Trondheim, Norway: Mar. Cybern., 2002.
- [10] M. Caccia, M. Bibuli, R. Bono, and G. Bruzzone, "Basic navigation, guidance and control of an unmanned surface vehicle," *Auton. Robots*, vol. 25, no. 4, pp. 349–365, 2008.
- [11] K. Pettersen and H. Nijmeijer, "Tracking control of an underactuated surface vessel," in *Proc. IEEE 37th Conf. Decis. Control*, 1998, pp. 4561–4566.
- [12] P. Encarnação and A. Pascoal, "Combined trajectory tracking and path following: An application to the coordinated control of autonomous marine craft," in *Proc. IEEE 40th Conf. Decis. Control*, 2001, pp. 964–969.
- [13] J. Ghommam and M. Saad, "Adaptive leader-follower formation control of underactuated surface vessels under asymmetric range and bearing constraints," *IEEE Trans. Veh. Technol.*, vol. 67, no. 2, pp. 852–865, Feb. 2018.
- [14] M. Breivik, V. Hovstein, and T. Fossen, "Ship formation control: A guided leader-follower approach," *IFAC Proc. Volumes*, vol. 41, no. 2, pp. 16008–16014, 2008.
- [15] W. Xie, B. Ma, T. Fernando, and H. H.-C. Iu, "A new formation control of multiple underactuated surface vessels," *Int. J. Control*, vol. 91, no. 5, pp. 1011–1022, 2018.
- [16] L. Chen, H. Hopman, and R. R. Negenborn, "Distributed model predictive control for cooperative floating object transport with multi-vessel systems," *Ocean Eng.*, vol. 191, 2019, Art. no. 106515.
- [17] L. Chen, H. Hopman, and R. R. Negenborn, "Distributed model predictive control for vessel train formations of cooperative multi-vessel systems," *Transp. Res. Part C, Emerg. Technol.*, vol. 92, pp. 101–118, 2018.
- [18] T. I. Fossen, M. Breivik, and R. Skjetne, "Line-of-sight path following of underactuated marine craft," *IFAC Proc. Volumes*, vol. 36, no. 21, pp. 211–216, 2003.
- [19] M. Breivik and T. I. Fossen, "Path following of straight lines and circles for marine surface vessels," *IFAC Proc. Volumes*, vol. 37, no. 10, pp. 65–70, 2004.
- [20] T. Fossen, "Line-of-sight path-following control utilizing an extended Kalman filter for estimation of speed and course over ground from GNSS positions," *Mar. Sci. Technol.*, vol. 27, pp. 806–813, 2022.
- [21] M. Bibuli, M. Caccia, L. Lapiere, and G. Bruzzone, "Guidance of unmanned surface vehicles: Experiments in vehicle following," *IEEE Robot. Automat. Mag.*, vol. 19, no. 3, pp. 92–102, Sep. 2012.
- [22] M. Bibuli, G. Bruzzone, M. Caccia, and L. Lapiere, "Path-following algorithms and experiments for an unmanned surface vehicle," *J. Field Robot.*, vol. 26, no. 8, pp. 669–688, 2009.

- [23] S. Zhang, S. Yang, and X. Xiang, "Formation control of autonomous surface vehicle and experimental validation," *IFAC-PapersOnLine*, vol. 52, no. 24, pp. 278–282, 2019.
- [24] D. Belleter, J. Braga, and K. Pettersen, "Experimental verification of a coordinated path-following strategy for underactuated marine vehicles," *Front. Robot. AI*, vol. 6, 2019, Art. no. 35.
- [25] A. Franceschi, B. Piaggio, R. Tonelli, D. Villa, and M. Viviani, "Assessment of the manoeuvrability characteristics of a twin shaft naval vessel using an open-source CFD code," *J. Mar. Sci. Eng.*, vol. 9, no. 6, 2021, Art. no. 665.
- [26] A. Franceschi, B. Piaggio, D. Villa, and M. Viviani, "Development and assessment of CFD methods to calculate propeller and hull impact on the rudder inflow for a twin-screw ship," *Appl. Ocean Res.*, vol. 125, Art. no. 103227.
- [27] A. Carchen, S. Turkmen, B. Piaggio, W. Shi, N. Sasaki, and M. Atlar, "Investigation of the manoeuvrability characteristics of a gate rudder system using numerical, experimental, and full-scale techniques," *Appl. Ocean Res.*, vol. 106, 2021, Art. no. 102419.
- [28] M. Martelli, D. Villa, M. Viviani, S. Donnarumma, and M. Figari, "The use of computational fluid dynamic technique in ship control design," *Ships Offshore Struct.*, vol. 16, no. 1, pp. 31–45, 2021.
- [29] M. Breivik, V. Hovstein, and T. Fossen, "Straight-line target tracking for unmanned surface vehicles," *Model. Identification Control*, vol. 29, no. 4, pp. 131–149, 2008.
- [30] A. Alessandri et al., "System control design of autopilot and speed pilot for a patrol vessel by using LMIs," in *Towards Green Mar. Technol. Transport Proc. 16th Int. Cong. Int. Maritime Assoc. Mediterranean*, 2015, pp. 577–583.
- [31] S. Donnarumma, L. Zaccarian, A. Alessandri, and S. Vignolo, "Anti-windup synthesis of heading and speed regulators for ship control with actuator saturation," in *Proc. Eur. Control Conf.*, 2016, pp. 1284–1290.
- [32] B. Piaggio, M. Viviani, M. Martelli, and M. Figari, "Z-drive escort tug manoeuvrability model and simulation, Part II: A full-scale validation," *Ocean Eng.*, vol. 259, 2022, Art. no. 111881.
- [33] B. Piaggio, M. Viviani, and M. Martelli, "Escort tug hydrodynamic forces estimation in a design framework: From model test to manoeuvrability simulation," in *Proc. Int. Conf. Offshore Mechanics Arctic Eng.*, 2018, Art. no. V11BT12A008.
- [34] B. Piaggio, "Azimuth-drive escort tug manoeuvrability model, simulation and control," Ph.D. dissertation, Università di Genova, Genoa, Italy, 2020.
- [35] A. Haseltalab and R. R. Negenborn, "Model predictive maneuvering control and energy management for all-electric autonomous ships," *Appl. Energy*, vol. 251, 2019, Art. no. 113308.
- [36] B. Piaggio, D. Villa, and M. Viviani, "Numerical analysis of escort tug manoeuvrability characteristics," *Appl. Ocean Res.*, vol. 97, 2020, Art. no. 102075.
- [37] B. Piaggio, D. Villa, M. Viviani, and M. Figari, "Numerical analysis of escort tug manoeuvrability characteristics – Part II: The skeg effect," *Appl. Ocean Res.*, vol. 100, 2020, Art. no. 102199.
- [38] T. Fossen, *Handbook of Marine Craft Hydrodynamics and Motion Control*. Hoboken, NJ, USA: Wiley, 2011.
- [39] A. Alessandri, S. Donnarumma, M. Martelli, and S. Vignolo, "Motion control for autonomous navigation in blue and narrow waters using switched controllers," *J. Mar. Sci. Eng.*, vol. 7, no. 6, 2019, Art. no. 196.
- [40] B. Piaggio, V. Garofano, S. Donnarumma, A. Alessandri, R. R. Negenborn, and M. Martelli, "Follow-the-leader control strategy for azimuth propulsion system on surface vessels," in *Proc. Int. Conf. Ship Control Syst. Symp. Vol. 1 - 2020, 15th Int. Naval Eng. Conf. Exhibit. Incorporat. Int. Ship Control Syst. Symp. (INEC/iSCSS)*, Oct. 5–9, 2020.



**Benedetto Piaggio** received the Ph.D. degree in naval architecture and marine engineering from the University of Genoa, Genoa, Italy, in 2020.

He is currently an Assistant Professor with the University of Genoa. In 2019, he was a Visiting Researcher with ResearchLab on Autonomous Shipping (RAS), Delft University of Technology, Delft, The Netherlands. His research interests include surface vessel and underwater vehicle hydrodynamic modeling, manoeuvrability simulation, navigation control, escort tug manoeuvrability, and towing cooperative dynamics.



**Vittorio Garofano** received the M.Sc. degree in mechatronic engineering from the Polytechnic University of Turin, Turin, Italy, in 2015.

He is currently a Research Support Engineer in the section of transport engineering and logistics with the Delft University of Technology, Delft, The Netherlands, and, where, since 2019, he has been the Technical Developer of the research projects carried out in the ResearchLab on Autonomous Shipping (RAS). His research interests include applied control theory, adaptive and robust control, formation and multiagent control algorithms, and real-time embedded software for autonomous ship system.



**Silvia Donnarumma** received the Ph.D. degree in mathematical engineering and simulation from the University of Genoa, Genoa, Italy, in 2016.

After a period at the University of Trento, Trento, Italy, she got a Postdoc Position with the University of Genoa, where she is currently an Assistant Professor. Her research interests include the study and application of nonlinear control techniques, based on hybrid approaches (with resets) and on convex optimization techniques based on LMIs for the synthesis of feedback control systems, dynamic positioning system, control with actuator saturations, and automatic steering.



**Angelo Alessandri** (Senior Member, IEEE) received the Ph.D. degree in electronics and computer engineering from the University of Genoa, Genoa, Italy, in 1996.

From 1996 to 2005, he was a Research Scientist with the National Research Council of Italy, Genoa. In 2006, he joined the University of Genoa, where he is currently a Full Professor with the Department of Mechanical, Energetics, Management, and Transportation Engineering. His research interests include state observers, moving-horizon estimation, and optimal control.

optimal control.

Dr. Alessandri was the Editor of the *International Journal of Adaptive Control and Signal Processing* and an Associate Editor for the *EUCA European Journal of Control* and of the IFAC journal *Automatica*.



**Rudy R. Negenborn** received the Ph.D. degree in distributed control from the Delft University of Technology, Delft, The Netherlands, in 2007. He is currently a Full Professor on multimachine operations and logistics, Head of Section Transport Engineering and Logistics with the Delft University of Technology, Delft, The Netherlands. He has authored or coauthored more than 200 papers in the area of his research fields, which include massive introduction of sensing, computation, communication technologies, and automatic control and coordination of transport technology (including autonomous vessels).



**Michele Martelli** received the B.S., M.S., and Ph.D. degrees in marine engineering and naval architecture from the University of Genoa, Genoa, Italy, in 2006, 2009, and 2013, respectively.

He is currently an Associate Professor with the University of Genoa, Genoa, Italy. Since 2010, he has been actively working on several research projects, funded by both private and public companies. He is a coauthor of more than 60 scientific papers. His research focuses on the study of the dynamics of the propulsion plant and its control system.